doi:10.1006/jmbi.2000.3711 available online at http://www.idealibrary.com on IDEAL® J. Mol. Biol. (2000) 298, 833–840

JMB

In-situ Atomic Force Microscopy Study of β-Amyloid Fibrillization

H. K. L. Blackley[1], G. H. W. Sanders[1], M. C. Davies[1], C. J. Roberts[1] S. J. B. Tendler[1]* and M. J. Wilkinson[2]

[1]*Laboratory of Biophysics and Surface Analysis, School of Pharmaceutical Sciences University of Nottingham University Park, Nottingham NG7 2RD, UK*

[2]*Microscopy, Analytical Sciences, SmithKline Beecham Pharmaceuticals, NFSP, Third Avenue, Harlow, CM19 5AW UK*

**Corresponding author*

We report the use of atomic force microscopy to observe the initial stages of β-amyloid fibrillization *in situ*. The growth of individual β-amyloid protofibrils on a mica substrate was followed over several hours. The first *in situ* visualization of protofibril formation from single aggregate units of β-amyloid is reported. The growth of these protofibrils through the subsequent addition of these aggregate units is also observed. Growth of the protofibrils is bi-directional and the outgrowth of protofibrils from a common amyloid/heterogeneous core is also observed. Elongation also occurred by the addition of protofibrils from solution. This data provides an exciting insight into the early stages of β-amyloid fibrillization and can be used to enhance the understanding of the mechanism(s) by which β-amyloid fibrillizes and may consequently enable inhibition of one or more stages of fibrillization as a potential therapeutic strategy.

Keywords: β-amyloid; Alzheimer's disease; atomic force microscopy; fibril formation; protofibril

Introduction

One of the major histopathological hallmarks of Alzheimer's disease is the abundant and progressive formation of amyloid plaques. These deposits consist primarily of β-amyloid; a 39-43 amino acid peptide (Glenner & Wong, 1984) polymerized as insoluble fibrils. Electron microscopy has shown these fibrils to be 6-10 nm in diameter (Merz *et al.*, 1983; Narang, 1980). X-ray diffraction (Kirschner *et al.*, 1986) has revealed that the β-amyloid peptide adopts a cross-β sheet conformation within the fibril. Thus the axis of the fibril is perpendicular to the polypeptide strand and parallel to the orientation of the hydrogen bonds. Fibrils formed *in vitro*, from synthetic β-amyloid, are ultrastructurally similar to the *in vivo* fibrils (Kirschner *et al.*, 1987).

Soluble β-amyloid peptide is secreted normally from cultured cells and is present in cerebrospinal fluid at nanomolar concentrations (Busciglio *et al.*, 1993; Haass *et al.*, 1992; Seubert *et al.*, 1992; Shoji *et al.*, 1992). Therefore there is great interest in understanding the mechanism(s) by which this soluble peptide converts into the insoluble fibrils found within the amyloid plaques. The causative role of these β-amyloid deposits in Alzheimer's disease has not definitively been established, but sufficient evidence exists to support the hypothesis that β-amyloid is pivotal to the aetiology of the disease. Earlier work suggested that the neurotoxic species was the mature β-amyloid fibril (Howlett *et al.*, 1995; Pike *et al.*, 1991, 1993; Seilheimer *et al.*, 1997), but more recent studies are indicating the existence of amyloid-derived diffusable ligands that are also neurotoxic (Lambert *et al.*, 1998). These findings present potential targets for therapeutic intervention at all stages of β-amyloid fibrillization.

In vitro work has suggested that β-amyloid fibrillization proceeds *via* two distinct stages; nucleation and elongation (Jarrett *et al.*, 1993; Lomakin *et al.*, 1996). During nucleation a series of thermodynamically unfavourable steps lead to the formation of a stable nucleus of undefined size. Identification of small particles of a size equivalent to the diameter of a β-amyloid fibril (Lomakin *et al.*, 1996) has indicated that such nuclei could be very short fibrils. Heterogeneous nucleation, with non-amyloido-

Present address: G. H. W. Sanders, Astra Zeneca/SmithKline Beecham Centre for Analytical Sciences, Department of Chemistry, Imperial College of Science, Technology and Medicine, London, SW7 2AY, UK.

Abbreviations used: AFM, atomic force microscopy.

E-mail address of the corresponding author: saul.tendler@nottingham.ac.uk

0022-2836/00/050833–8 $35.00/0

genic seed material may also occur. Subsequent elongation of the fibrils is thought to be first order; it proceeds at a rate directly proportional to the β-amyloid concentration (Jarrett *et al.*, 1993; Esler *et al.*, 1996; Naiki & Nakakuki, 1996).

A model of β-amyloid fibrillization has been proposed whereby an intermediate of fibrillization develops from these fibril nuclei by the addition of monomers (Walsh *et al.*, 1997). This intermediate structure is termed a protofibril and has been identified by a number of groups. Electron microscopy of β-amyloid protofibrils yielded structures 6-10 nm in diameter and 5-160 nm in length (Walsh *et al.*, 1997). *Ex situ* atomic force microscopy (AFM) data also supports the existence of protofibrils. By sampling β-amyloid over a period of time, protofibrils approximately 3 nm in diameter and 20-70 nm in length were seen to appear and then later disappear to be replaced by more typical mature fibrils (Harper *et al.*, 1997a). This suggests that the protofibril is an intermediate of fibrillization. Subsequent work revealed that the conversion of protofibrils to fibrils could be seeded by preformed fibrils (Harper *et al.*, 1997b). More recent *ex situ* AFM experiments have also revealed that protofibril elongation, like fibril elongation, is first order (Harper *et al.*, 1999). In addition, the substructure of the protofibril has been clearly visualized by AFM. Immobilizing the protein species to a flat gold surface using an alkyl thiol self-assembled monolayer (Blackley *et al.*, 1999) revealed protofibrils of less than 300 nm in length, clearly comprising of individual aggregates of β-amyloid.

Recent work has used AFM to investigate the assembly dynamics of several amyloidogenic proteins. The first of these *in situ* experiments observed the growth of individual protofibrils and fibrils of amylin on a mica surface over a period of several hours (Goldsbury *et al.*, 1999). Here, the protofibril growth was seen to be bi-directional and to proceed at an elongation rate of 1.1(±0.5) nm/minute. The aggregation of β-amyloid in contact with two model surfaces has also been investigated (Kowalewski & Holtzman, 1999). On hydrophilic mica the β-amyloid formed particulate aggregates of average height 5-6 nm. At high β-amyloid concentrations (500 μM) these were seen to assemble into linear structures resembling β-amyloid protofibrils. However on hydrophobic graphite the β-amyloid formed uniform elongated sheets, approximately 1 nm in height.

Here, we report the use of AFM to observe the initial stages of β-amyloid fibrillization *in situ.* The unique capacity of AFM to produce high-resolution images of a sample immersed in solution enabled the development of a population of β-amyloid fibrils to be followed over time. Tapping mode imaging was employed; this mode virtually eliminates lateral forces between the probe and the sample and allows the observation of the weakly adsorbed protein without modification of the mica substrate. Thus the *in situ* visualization of protofibril formation from single aggregate units of β-amyloid has been investigated. The subsequent growth of these protofibrils by the further addition of these aggregates has also been studied. The information obtained here can be used to enhance the understanding of the mechanism(s) by which β-amyloid fibrillizes.

Results

Development of a population of β-amyloid fibrils over time

The development of a population of β-amyloid fibrils over time is displayed in Figure 1. This was achieved by repeatedly imaging the same 13.5 μm square area of mica over time. Figure 1(a), taken 30 minutes after the start of incubation of the β-amyloid, displays a population made up of aggregates, protofibrils and short fibrils. In Figure 1(b), taken later at 80 minutes, a more dense deposition of β-amyloid material is apparent. Protofibrils and fibrils present on the mica at earlier time points have grown, whilst others have appeared on the surface from the bulk solution. Additionally some of the β-amyloid aggregates have developed into protofibrils. These processes have continued over the next 55 minutes as illustrated in Figure 1(c).

Statistical investigation of this population over a large series of images shows a minimal increase in the total number of β-amyloid aggregates (height > 1 nm) over time. This is illustrated in Figure 2(a). This minimal increase is unlikely to be due to saturation of the mica surface, as preliminary experiments at higher β-amyloid concentrations showed a far greater density of protein deposition (data not shown). A general term for these aggregates, single unit aggregates, will be used throughout this paper. However a pronounced increase in the number of large aggregates (height > 5 nm) over time is also observed as is shown in Figure 2(b). This data suggests that the single unit aggregates of β-amyloid may be coalescing on the mica and that there is an ongoing adsorption/desorption of material at the solid/liquid interface. Similar trends were observed with other data sets.

Protofibril development

Figure 3(a) and (b) show the formation and growth of a protofibril from single aggregate units of β-amyloid over a time span of approximately two hours. The single aggregate units are 83.3(±18.2) nm wide and 4.5(±2.8) nm high ($n = 80$). The initial fusion of two of these entities occurs at different times throughout the imaging. Figure 3(a) is a 1 μm × 1 μm image, digitally zoomed in from a 13.5 μm × 13.5 μm scan. In the first image, collected an hour after the start of incubation, two single aggregate units of β-amyloid are imaged separately but in close proximity. Nearly 40 minutes later, by the third image, these two

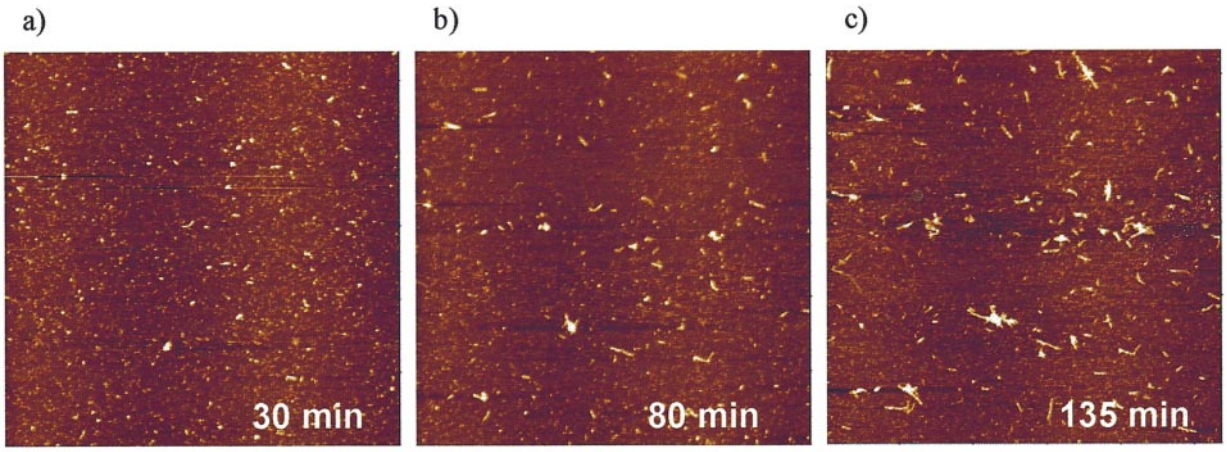

Figure 1. Fibrillization of β-amyloid on mica. Tapping mode AFM images acquired *in situ* in a 50 μg/ml solution of β-amyloid in Tris. The images are of essentially the same 13.5 μm × 13.5 μm area although a slight amount of drift has occurred throughout the experiment. A common point easily visible on all three images is the large aggregate in the bottom left-hand quarter of the scan. Over time aggregates, protofibrils and fibrils of β-amyloid grow on the mica surface. Preformed fibrils from the bulk solution also appear.

units are fused together and a third unit has added onto the (now) protofibrillar structure. At the end of this series of images the structure is far more linear, although the single aggregate origin is still obvious from the axial cross-section. Figure 3(b), again a digitally zoomed 1 μm × 1 μm image, contains another example of this process. Four single aggregate units of β-amyloid are fused together by the end of the series of images. It is interesting to note that a third aggregate unit adds at 80 minutes. Eight minutes later the size of this structure has apparently increased. This could be due to a change in the orientation of the aggregate on the mica substrate or to the addition of β-amyloid monomers.

Figure 3(c) (a digitally zoomed 1 μm × 1 μm image) contains additional data supporting the proposition that protofibril elongation can occur by the addition of single aggregate units. The protofibril present in the first image displayed in Figure 3(c) elongates by the addition of two single aggregate units to the top end of the structure. This is apparent nine minutes later as shown in the second image of the sequence. Eight minutes later, as illustrated in the third image, elongation of the bottom end of the protofibril has occurred by an identical process. Thus elongation of protofibrils can be seen to be bi-directional.

Development of multiple β-amyloid protofibrils from a common core

Another phenomenon observed is the development of multiple β-amyloid protofibrils from a common core. This is apparent in Figure 4, a digitally zoomed 2.5 μm × 2.5 μm image. The nuclea-

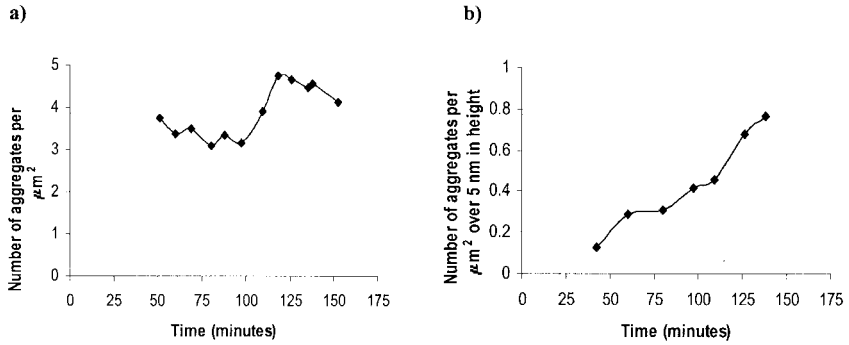

Figure 2. (a) A graph illustrating that the number of β-amyloid aggregates (height >1 nm) per unit area of mica is fairly constant throughout the experiment. (b) A graph showing a pronounced increase in the number of aggregates of height >5 nm per unit area during the experiment. The data was obtained by using thresholding software as detailed in Materials and Methods.

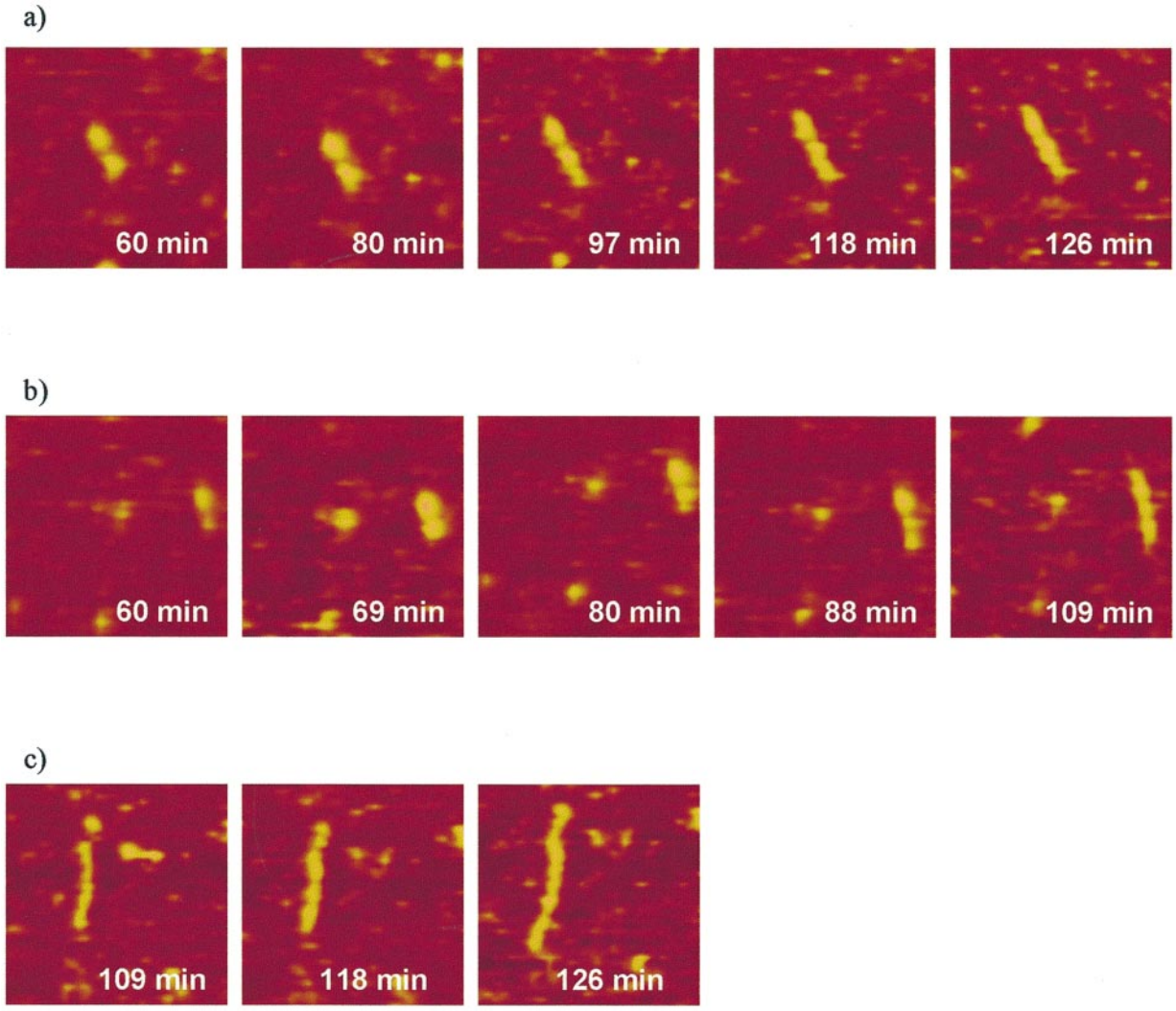

Figure 3. The consecutive addition of aggregates of β-amyloid to form protofibrils. The images are 1 μm × 1 μm in size, digitally zoomed in from a 13.5 μm × 13.5 μm scan. (a) and (b) The formation of protofibrils from two single aggregate units of β-amyloid and subsequent elongation by the addition of further aggregate units of β-amyloid. (c) The bi-directional elongation of a β-amyloid protofibril by the addition of aggregate units of β-amyloid.

tion point, initially 250 nm wide as displayed in Figure 4(a), may be amyloidogenic or heterogeneous in origin. Twenty minutes later, as observed in Figure 4(b), a protofibril is developing as an offshoot by the addition of single aggregate units of β-amyloid. An hour after the start of the experiment, as displayed in Figure 4(c), another emerging protofibril is apparent. At 88 minutes, as illustrated by Figure 4(f), four protofibrils are radiating from the central core. During the next 20 minutes that elapse between the capture of the image displayed in Figure 4(f) and Figure 4(g), a pre-existing protofibril appears to add from solution. This suggests that protofibril elongation can occur by both the addition of pre-existing protofibrils and single aggregate units of β-amyloid.

Protofibril elongation rates

Here, the formation of a protofibril is defined as the fusion of two single aggregate units of β-amyloid. This definition of a protofibril is used as the starting point for all reported elongation measurements. No change in morphology, for example increase in width, was observed over the course of these measurements. Such a change would be indicative of a transition of protofibril to fibril.

Elongation rates for the protofibrils have been calculated ($n = 40$) and are found to vary considerably as shown in Figure 5 (only part of the data displayed). The elongation rate varies from approximately 1 nm/minute to 10 nm/minute. This is probably due in part to the visualization of

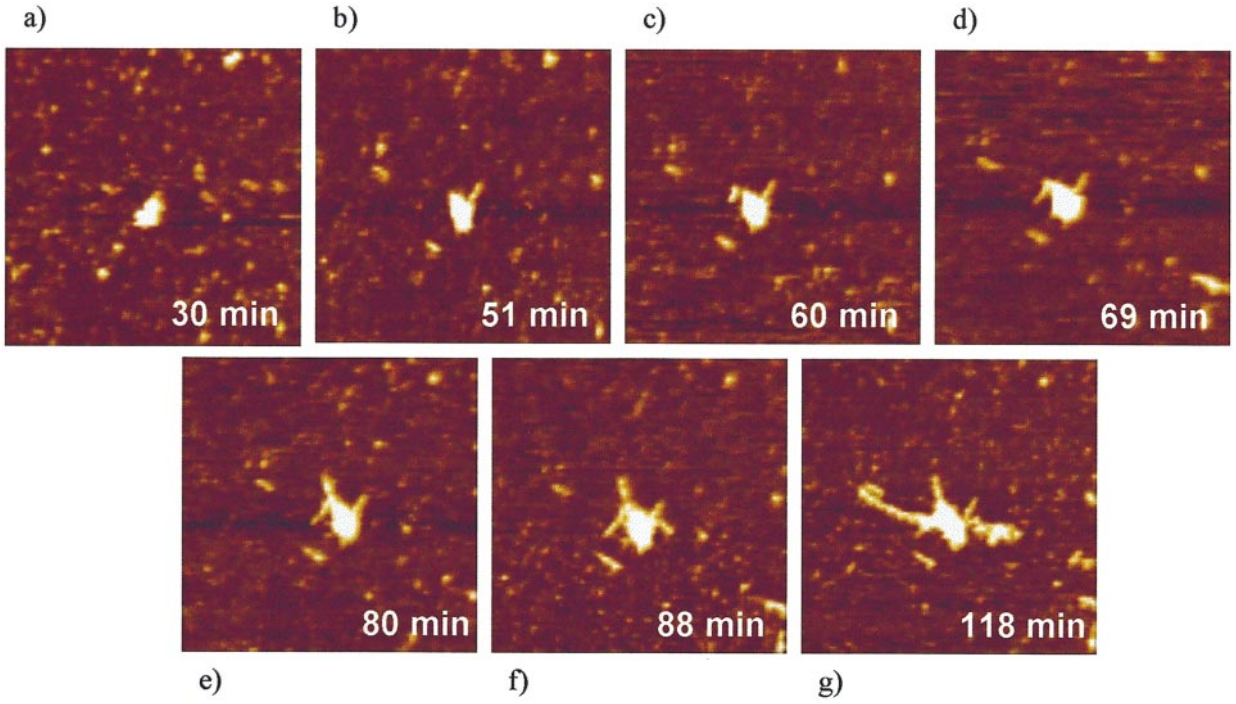

Figure 4. A series of AFM images depicting the development of multiple β-amyloid protofibrils from a common core. Elongation occurs by addition of β-amyloid aggregates and, between 88 and 118 minutes, by the addition of a preformed protofibril from the solution. The image size is 2.5 μm × 2.5 μm, digitally zoomed in from a 13.5 μm × 13.5 μm scan.

the two mechanisms of protofibril elongation (addition of single aggregate units and pre-existing protofibrils). Monte Carlo simulations give an estimate for the solid volume of an individual β-amyloid molecule when packed into a protofibril (personal communication, Ashley George). This value is approximately 6.04 nm^3 (larger than 4.269 nm^3 calculated for an *in vacuo* β-amyloid peptide). A cylindrical structure for the protofibril can be assumed and the protofibril height taken as approximately 4.5 nm (from measurements on this data set). It can then be calculated that there are approximately 2.5 peptide monomers per nm of protofibril length. Therefore the elongation rates seen here correspond to the addition of 2.5-25 monomers per minute.

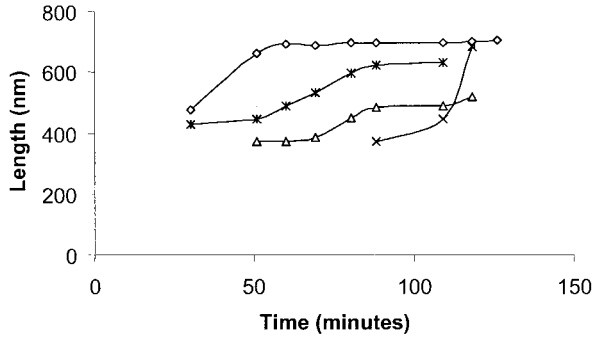

Figure 5. This graph illustrates the variation in elongation rates of the protofibrils. It can be seen that they develop at different times over the course of the imaging and that the rate of elongation is not uniform for each protofibril.

Discussion

Here, *in situ* AFM has been used to observe the formation of protofibrils from single aggregate units of β-amyloid. The single aggregate units are 83.3(±18.2) nm wide and 4.5(±2.8) nm high, measurements which differ from those made in *ex situ* experiments where similar features are found to be 21.3(±3.0) nm wide and 2.5(±0.9) nm high. However the height of these single aggregate units of β-amyloid is similar to that obtained in other *in situ* experiments where the height of such features was 5-6 nm (Kowalewski & Holtzman, 1999). There may be several reasons for this disparity in dimensions that can sometimes occur between structures measured in air (*ex situ*) and in liquid (*in situ*). In an aqueous environment, the β-amyloid aggregates will be fully hydrated with the hydrophilic N terminus of the peptide (residues 1 to 29) exposed on the outer surface of the aggregate. This could lead to the β-amyloid aggregates adopting an extended conformation on the mica substrate

and the increased dimensions seen. It must also be considered that the use of the silicone O-ring and liquid cell can lead to anomalous lateral measurements with the AFM (Neff *et al*., 1999). Electrostatic double layer forces between the tip and sample also contribute to the recorded height in liquid and can lead to the measurement of heights differing greatly from those recorded using other techniques (Muller & Engel, 1997). *Ex situ* measurements will be far more dependent on environmental factors, such as humidity.

In aqueous buffers the β-amyloid single unit aggregates and protofibrils are only loosely associated with the mica substrate *via* electrostatic interactions. This can be seen by the fact that some single aggregate units of β-amyloid desorb from the mica surface during imaging whilst others exhibit considerable lateral mobility. This is most clearly seen when two single aggregate units come together to form a protofibril. It is the very fact that the protein molecules are so weakly attached to the mica surface that allows the formation and growth of the protofibrils to be observed. Other studies (data not shown), where the β-amyloid is chemically immobilized to a gold surface, show minimal evidence of fibril growth. Therefore this mica/Tris buffer system more closely mimics the situation *in vivo*.

The development of the β-amyloid protofibrils observed here has important implications for the possible mechanism(s) of fibrillization of this peptide. It is evident that the formation of protofibrils occurs in the first instance by the joining of two single aggregate units of β-amyloid. These aggregate units are of yet undefined mass. Elongation of these protofibrils proceeds by the addition of further aggregate units and protofibrils. Protofibrils observed here, comprising of individual aggregate units, are of lengths of up to 1 μm, clearly in excess of those recorded by other groups (Walsh *et al*., 1997; Harper *et al*., 1997a, 1999). The range in protofibril length is also great, varying from 200 nm to 1 μm. However the height of these protofibrils (approximately 4.5 nm) is comparable to measurements obtained by *ex situ* AFM (Harper *et al*., 1999) and electron microscopy (Walsh *et al*., 1997) suggesting that they may be the same structures. Development of the protofibrils into mature fibrils may then occur by the further addition of single aggregate units of β-amyloid, β-amyloid monomers and other protofibrils. Winding of protofibrils and conformational change may also be involved (Harper *et al*., 1997a). These possible mechanisms of fibrillization are outlined in Figure 6.

It is thought that the low concentration of β-amyloid used (50 μg/ml) and the fact that the assembly of β-amyloid is constrained by the mica substrate enabled the observation of such a large population of single aggregate units and protofibrils. This phenomenon has also been observed during *in situ* AFM of amylin fibrillization (Goldsbury *et al*., 1999). Single aggregate units and protofibrils are observed far less frequently at similar time points when using *ex situ* AFM (data not

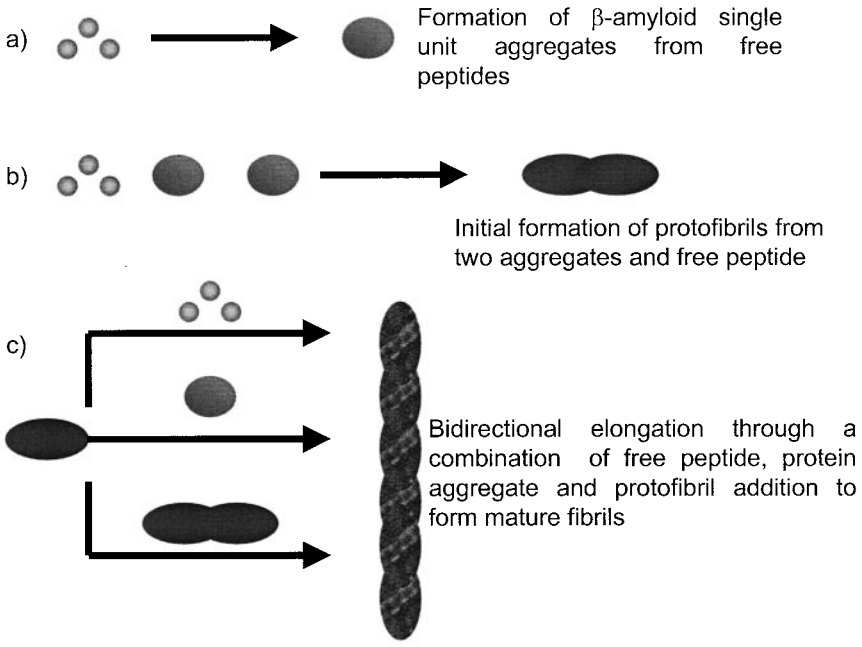

Figure 6. A schematic outlining a possible mechanism for the fibrillization of β-amyloid. (a) A single aggregate unit forms from β-amyloid peptide monomers. These aggregate units then assemble together, possibly with monomer as well, to form protofibrils as in (b). Elongation to form mature fibrils occurs by addition of monomer, aggregate or protofibril, or any combination of these as in (c). Protofibril winding and conformational change may also be involved in (c).

shown). During these *ex situ* experiments samples are prepared at various stages of the fibrillization process. Protofibrils are seen to disappear over the longer time courses, being replaced by more mature fibrils. This supports the suggestion that these short fibrils are some sort of intermediate of the β-amyloid fibrillization process. The *in situ* AFM experiments may not be conducted over such long time periods due to problems with protein adsorbing to the tip and impairing imaging.

The data displayed here demonstrates the applicability of using AFM to follow real-time processes *in situ.* It has been possible to observe, for the first time, one of the early stages of protofibril formation, the joining of two single aggregate units of β-amyloid. This is of particular importance as evidence is now available to suggest that these aggregate species are also neurotoxic (Lambert *et al.*, 1998). Now that AFM can be used to observe this critical event in the pathogenesis of Alzheimer's disease, it may be possible to identify conditions, which either activate or inhibit the β-amyloid fibrillization process. The ability to study individual fibrils will enable us to establish if these compounds are targeting higher or lower order fibrillar species. Such *in vitro* studies will contribute to understanding how β-amyloid fibrils behave *in vivo* and to elucidating their role in the aetiology of Alzheimer's disease.

Materials and Methods

Sample preparation

β(1-40) amyloid was purchased as a lyophilized solid from California Peptide Research (batch ME1041, CA). Mica was purchased from Agar Scientific (Essex). Aqueous solutions of β-amyloid were prepared by diluting 1 mg/ml in deionized, distilled water into Tris buffer (pH 7.0, 50 mM) at a concentration of 50 μg/ml. Solutions were added to the liquid cell over the freshly cleaved mica substrate, after a few minutes incubation.

AFM imaging conditions

AFM imaging was performed on a Nanoscope IIIa MultiMode scanning probe workstation (Digital Instruments, Santa Barbara, CA) using an ''E'' type scanner with xy range of 15 μm. The standard fluid cell attachment was used, with a silicone O-ring compressed against the sample to obtain a good seal. Short, narrow legged silicon nitride cantilevers (nominal spring constant 0.032 N/m) were used. The best imaging results were obtained using a tapping frequency in the range 9-10 kHz. Typical scan rates were between 1-2 Hz. Drive amplitudes were in the range 150-300 mV. The original images were sampled at a resolution of 512 × 512 and imaging was performed at room temperature. In all presented Figures the height information is represented by contrast difference, with the lighter shades corresponding to the higher features.

Analysis of AFM images

Size distribution of aggregates of β-amyloid on the mica were determined with the aid of SPM ImageMagic (web site address http://www.geocities. com/SiliconValley/Network/6216/). The length of the fibrillar features was determined using the section analysis option of the Nanoscope image analysis software. Height measurements were taken at peak heights as the protofibrils exhibited quite distinct axial periodicity and a variation in z of >2 nm in some cases.

Acknowledgements

H.K.L.B. acknowledges the financial support of a BBSRC CASE award with SmithKline Beecham Pharmaceuticals. G.H.W.S. thanks the BBSRC for postdoctoral support.

References

Blackley, H. K. L., Patel, N., Davies, M. C., Roberts, C. J., Tendler, S. J. B., Williams, P. M. & Wilkinson, M. J. (1999). Morphological development of β(1-40) amyloid fibrils. *Exp. Neurol.* **158**, 437-443.

Busciglio, J., Gabuzda, D. H., Matsudaira, P. & Yankner, B. A. (1993). Generation of β-amyloid in the secretory pathway in neuronal and non-neuronal cells. *Proc. Natl Acad. Sci. USA,* **90**, 2092-2096.

Esler, W. P., Stimson, E. R., Ghilardi, J. R., Vinters, H. V., Lee, J. P., Mantyh, P. W. & Maggio, J. E. (1996). *In vitro* growth of Alzheimer's disease β-amyloid plaques displays first-order kinetics. *Biochemistry,* **35**, 749-757.

Glenner, G. G. & Wong, C. W. (1984). Alzheimer's disease: initial report of the purification and characterization of a novel cerebrovascular amyloid protein. *Biochem. Biophys. Res. Commun.* **120**, 885-890.

Goldsbury, C., Kistler, J., Aebi, U., Arvinte, T. & Cooper, C. J. S. (1999). Watching amyloid fibrils grow by time-lapse atomic force microscopy. *J. Mol. Biol.* **285**, 33-39.

Haass, C., Schlossmacher, M. G., Hung, A. Y., Vigo-Pelfrey, C., Mellon, A., Ostaszewski, B. L., Lieberburg, I., Koo, E. H., Schenk, D., Teplow, D. B. & Selkoe, D. (1992). Amyloid beta-peptide is produced by cultured cells during normal metabolism. *Nature,* **359**, 322-325.

Harper, J. D., Wong, S. S., Lieber, C. M. & Lansbury, P. T. (1997a). Atomic force microscopy imaging of seeded fibril formation and fibril branching by the Alzheimer's disease amyloid-β protein. *Chem. Biol.* **4**, 951-959.

Harper, J. D., Wong, S. S., Lieber, C. M. & Lansbury, P. T. (1997b). Observation of metastable Aβ amyloid protofibrils by atomic force microscopy. *Chem. Biol.* **4**, 119-125.

Harper, J. D., Wong, S. S., Lieber, C. M. & Lansbury, P. T. (1999). Assembly of Aβ-amyloid protofibrils: an *in vitro* model for a possible early event in Alzheimer's disease. *Biochemistry,* **38**, 8972-8980.

Howlett, D. R., Jennings, K. H., Lee, D. C., Clark, M. S. G., Brown, F., Wetzel, R., Wood, S. J., Camilleri, P. & Roberts, G. W. (1995). Aggregation state and neurotoxic properties of Alzheimer β-amyloid peptide. *Neurodegeneration,* **4**, 23-32.

Jarrett, J. T., Berger, E. P. & Lansbury, P. T. (1993). The carboxy terminus of β-amyloid protein is critical for the seeding of amyloid formation: implications for the pathogenesis of Alzheimer's disease. *Biochemistry,* **32**, 4693-4697.

Kirschner, D. A., Abraham, C. & Selkoe, D. J. (1986). X-ray diffraction from intraneuronal paired helical filaments and extraneuronal amyloid fibers in Alzheimer-disease indicates cross-β conformation. *Proc. Natl Acad. Sci. USA,* **83**, 503-507.

Kirschner, D. A., Inouye, H., Duffy, L. K., Sinclair, A., Lind, M. & Selkoe, D. J. (1987). Synthetic peptide homologous to β protein from Alzheimer disease forms amyloid-like fibrils *in vitro*. *Proc. Natl Acad. Sci. USA,* **84**, 6953-6957.

Kowalewski, T. & Holtzman, D. M. (1999). *In situ* atomic force microscopy study of Alzheimer's β-amyloid peptide on different substrates: new insights into mechanism of β-sheet formation. *Proc. Natl Acad. Sci. USA,* **96**, 3688-3693.

Lambert, M. P., Barlow, A. K., Chromy, B. A., Edwards, C., Freed, R., Liosatos, M., Morgan, T. E., Rozovsky, I., Trommer, B., Viola, K. L., Wals, P., Zhang, C., Finch, C. E., Krafft, G. A. & Klein, W. L. (1998). Diffusable, nonfibrillar ligands derived from $A\beta_{1\text{-}42}$ are potent central nervous system neurotoxins. *Proc. Natl Acad. Sci. USA,* **95**, 6448-6453.

Lomakin, A., Chung, D. S., Benedek, G. B., Kirschner, D. A. & Teplow, D. B. (1996). On the nucleation and growth of amyloid β-protein fibrils: detection of nuclei and quantitation of rate constants. *Proc. Natl Acad. Sci. USA,* **93**, 1125-1129.

Merz, P. A., Wisniewski, H. M., Somerville, R. A., Bobin, S. A., Masters, C. L. & Iqbal, K. (1983). Ultrastructural morphology of amyloid fibrils from neuritic and amyloid plaques. *Acta Neuropathol.* **60**, 113-124.

Muller, D. J. & Engel, A. (1997). The height of biomolecules measured with the atomic force microscope depends on electrostatic interactions. *Biophys. J.* **73**, 1633-1644.

Naiki, H. & Nakakuki, K. (1996). First-order kinetic model of Alzheimer's β-amyloid fibril extension *in vitro*. *Lab. Invest.* **74**, 374-383.

Narang, H. K. (1980). High-resolution electron microscopic analysis of the amyloid fibril in Alzheimer's disease. *J. Neuropathol. Exp. Neurol.* **39**, 621-631.

Neff, G. A., Gragson, D. E., Short, D. A. & Baker, S. M. (1999). Anomalous lateral size measurements by atomic force microscopy in a fluid cell. *Langmuir,* **15**, 2999-3002.

Pike, C. J., Walencewicz, A. J., Glabe, C. G. & Cotman, C. W. (1991). *In vitro* aging of β-amyloid protein causes peptide aggregation and neurotoxicity. *Brain Res.* **563**, 311-314.

Pike, C. J., Burdick, D., Walencewicz, A. J., Glabe, C. G. & Cotman, C. W. (1993). Neurodegeneration induced by β-amyloid peptides *in-vitro*: the role of peptide assembly state. *J. Neurosci.* **13**, 1676-1687.

Seilheimer, B., Bohrmann, B., Bondolfi, L., Muller, F., Stuber, D. & Dobeli, H. (1997). The toxicity of the Alzheimer's β-peptide correlates with a distinct fiber morphology. *J. Struct. Biol.* **119**, 59-71.

Seubert, P., Vigo-Pelfrey, C., Esch, F., Lee, M., Dovey, H., Davis, D., Sinha, S., Schlossmacher, M., Whaley, J., Swindlehurst, C., McCormack, R., Wolfert, R., Selkoe, D., Lieberburg, I. & Schenk, D. (1992). Isolation and quantification of soluble Alzheimer's β-peptide from biological fluids. *Nature,* **359**, 325-327.

Shoji, M., Golde, T. E., Ghiso, J., Cheung, T. T., Estus, S., Shaffer, L. M., Cai, X.-D., Mckay, D. M., Tintner, R., Frangione, B. & Younkin, S. G. (1992). Production of the Alzheimer amyloid β-protein by normal proteolytic processing. *Science,* **258**, 126-129.

Walsh, D. M., Lomakin, A., Benedek, G. B., Condron, M. M. & Teplow, D. B. (1997). Amyloid β-protein fibrillogenesis- Detection of a protofibrillar intermediate. *J. Biol. Chem.* **272**, 22364-22372.

Edited by M. F. Moody

(Received 19 November 1999; received in revised form 16 March 2000; accepted 21 March 2000)